

OFF-CRITICAL LOCAL HEIGHT PROBABILITIES ON A PLANE AND CRITICAL PARTITION FUNCTIONS ON A CYLINDER

OMAR FODA

ABSTRACT. We compute off-critical local height probabilities in regime-III restricted solid-on-solid models in a $4N$ -quadrant spiral geometry, with periodic boundary conditions in the angular direction, and fixed boundary conditions in the radial direction, as a function of N , the winding number of the spiral, and τ , the departure from criticality of the model, and observe that the result depends only on the product $N\tau$. In the limit $N \rightarrow 1$, $\tau \rightarrow \tau_0$, such that τ_0 is finite, we recover the off-critical local height probability on a plane, τ_0 -away from criticality. In the limit $N \rightarrow \infty$, $\tau \rightarrow 0$, such that $N\tau = \tau_0$ is finite, and following a conformal transformation, we obtain a critical partition function on a cylinder of aspect-ratio τ_0 . We conclude that the off-critical local height probability on a plane, τ_0 -away from criticality, is equal to a critical partition function on a cylinder of aspect-ratio τ_0 , in agreement with a result of Saleur and Bauer.

1. INTRODUCTION

1.1. Background. In 1987, Date, Jimbo, Miwa and Okado observed that (the essential part of) the *off-critical* local height probabilities in an important class of solved statistical mechanical models on a square lattice are characters of fully-degenerate, irreducible Virasoro highest-weight modules, and in 1989, Saleur and Bauer observed that the same Virasoro characters are *critical* partition functions of conformal field theories on a cylinder, if the departure from criticality in the off-critical local height probabilities of Date *et al.* is matched to the aspect-ratio of the cylinder. In 1991, the present author proposed an argument to explain (or at least to motivate) the observation of Saleur and Bauer. This argument appeared in a preprint form, but was not widely-circulated and was not published. The present note recalls this argument.

1.2. Outline of contents. In section **2**, we recall basic definitions related to the restricted solid-on-solid models of Andrews, Baxter and Forrester, and in **3**, we do the same for Baxter's corner transfer matrix method and local height probabilities. In **4**, we outline how the corner transfer matrix is used to compute off-critical local height probabilities on a plane, in the form of modular functions, and in **5**, we recall the re-writing of the off-critical local height probabilities in terms of affine and Virasoro characters¹. In **6**, we recall the results of pioneering works where critical partition functions on a cylinder with fixed boundary conditions are expressed in terms of Virasoro characters, then outline the approach of the present work. In **7**, we extend the regime-III restricted solid-on-solid local height probabilities to a $4N$ -quadrant spiral geometry, with $N = 2, 3, \dots$, and show that the result is the product of two factors, **A** and **B**, where **A** is a normalization that depends on N and on τ separately, and **B** carries the statistical

Key words and phrases. Local height probabilities, Restricted solid-on-solid models, Baxter's corner transfer matrix method, Critical partition functions, Virasoro characters.

¹ Sections **2–5** are descriptive guides to the original literature rather than a substitute for it. They contain just enough information, and notation, to allow the reader to follow the subsequent sections, and can be skipped by the expert reader.

mechanics of the local height probability and depends only on the product $N\tau$. We give up the normalization of the local height probabilities as probabilities for $N \neq 1$, rewrite them in terms of affine and Virasoro characters and formally set $N \in \mathbb{R}$. In **8**, we regularize the $4N$ -quadrant off-critical local height probability, and take $N \rightarrow \infty, \tau \rightarrow 0$, such that $N\tau$ is fixed. In the limit, **A** simplifies, while **B** remains *invariant*, and the system is critical on a spiral geometry with infinite winding number. Conformally transforming the spiral to a cylinder, we obtain a critical partition functions on a cylinder. In section **9**, we collect a number of comments.

1.3. Abbreviations. To simplify the presentation, we often use **1**. ‘local height probability’ for ‘off-critical local height probability on a plane’, as one normally computes the local height probabilities off-criticality and on a plane, unless otherwise specified, **2**. ‘Virasoro highest weight module’ for ‘fully-degenerate irreducible Virasoro highest-weight module’, since we focus on statistical mechanical models that reduce at criticality to minimal conformal field theories based on Virasoro, rather than higher rank algebras.

1.4. Notation. In a restricted solid-on-solid model $\mathcal{L}_{m,m+1}$, $m = 3, 4, \dots$, is the number of allowed heights. The parameter $\tau \in \mathbb{R}$ measures the departure of an off-critical system from criticality, and $\tau' = 1/\tau$. The off-critical restricted solid-on-solid model $\mathcal{L}_{m,m+1}$, $m = 3, 4, \dots$, is defined in terms of Boltzmann weights parameterized by elliptic theta functions. The nome of these theta functions is $p = e^{-2\pi\tau'}$. The local height probabilities, which are essentially Virasoro characters, are q -series in $q = e^{-4\pi\tau/(m+1)}$. When working on a spiral geometry of winding number N , we take the modular parameter τ , and consequently the nome p and its modular conjugate q , to depend on N , and τ_N, p_N and q_N .

2. RESTRICTED SOLID-ON-SOLID MODELS

We recall basic facts related to the restricted solid-on-solid models of Andrews, Baxter and Forrester.

2.1. The hard-square model. In [1, 2], Baxter solved the hard-square model on a square lattice, where nearest-neighbouring sites cannot be simultaneously occupied, and interactions are along the diagonals. The hard-hexagon model on a triangular lattice is recovered by taking the energy of the interactions along one of the two diagonals to be infinite, so that the two sites connected by that diagonal cannot be simultaneously occupied. If we think of the free/occupied sites as carrying a height variable $h = 0/1$, such that any two nearest-neighbouring state-variables h_i and h_{i+1} satisfy $h_i + h_{i+1} \leq 1$, the hard-square model is the first example of a solved restricted-solid-on-solid model.

2.2. The restricted solid-on-solid models. In [3], Andrews, Baxter and Forrester introduced an infinite series of statistical mechanical models with Boltzmann weights that satisfy the face-version of the Yang-Baxter equations, and that generalize the hard-square model. These are the restricted solid-on-solid models $\mathcal{L}_{m,m+1}$, $m \in (3, 4, \dots)$ ².

² Also called the Andrews-Baxter-Forrester models. The hard-square model is $\mathcal{L}_{4,5}$.

2.2.1. *The state variables.* Following [3], a restricted solid-on-solid model is a statistical mechanical system of interacting state-variables that are also called ‘heights’. Each state-variable h lives at the intersection of a horizontal line and a vertical line in the lattice, and takes values in a finite set of integers $h \in (1, 2, \dots, m)$, where $m \in \mathbb{N}$ characterizes the model. Adjacent state-variables differ by ± 1 . A configuration in the restricted solid-on-solid model $\mathcal{L}_{4,5}$ is shown in Figure 2.1.

2.2.2. *Remark.* The hard-square model with occupancies $(0, 1)$, such that nearest-neighbouring state-variables satisfy $h_i + h_{i+1} \leq 1$, is equivalent to the $\mathcal{L}_{4,5}$ model with occupancies $(1, 2, 3, 4)$, such that nearest-neighbouring state-variables satisfy $h_i + h_{i+1} = \pm 1$, because any linear sequence of the first type can be mapped to a sequence of the second type, up to an involution. For example, $(0, 0, 0, 1, 0, 1, 0, 0, 1, 0, 0)$ maps to $(2, 3, 2, 1, 2, 1, 2, 3, 4, 3, 2)$, and also to $(3, 2, 3, 4, 3, 4, 3, 2, 1, 2, 3)$, every configuration in the hard-square model corresponds to two configurations in the $\mathcal{L}_{4,5}$ model, and the partition function of the hard-square model is related to that of the $\mathcal{L}_{4,5}$ model as $Z_{hard \text{ hexagon}} = \frac{1}{2} Z_{4,5}$

2.2.3. *Notation.* Given the elliptic theta functions³,

$$(2.1) \quad \theta_1(\eta x, p) = 2 p^{\frac{1}{4}} \sin(\eta x) \prod_{n=1}^{\infty} (1 - 2 \cos(2 \eta x) p^{2n} + p^{4n}) (1 - p^{2n}),$$

$$\theta_4(\eta x, p) = \prod_{n=1}^{\infty} (1 - 2 \cos(2 \eta x) p^{2n-1} + p^{2n-2}) (1 - p^{2n}),$$

we define the bracket $[x, p]$, or simply $[x]$ as short-hand notation for the product,

$$(2.2) \quad [x, p] = [x] = \theta_1(\eta x, p) \theta_4(\eta x, p) =$$

$$2 p^{\frac{1}{4}} \sin(\eta x) \prod_{n=1}^{\infty} (1 - 2 \cos(2 \eta x) p^n + p^{2n}) (1 - p^{2n})^2$$

In the sequel, $\eta = \frac{\pi}{m+1}$ is the crossing parameter of the model $\mathcal{L}_{m,m+1}$, $p = e^{-2\pi/\tau}$ is the nome of the elliptic theta function, and modular parameter τ measures the departure of the model from criticality, in the sense that, in the limit $\tau \rightarrow 0$, $p \rightarrow 0$, the Boltzmann weights become trigonometric, and the model becomes critical⁴.

2.2.4. *Remark.* It is useful to note that $[x, p^2] = \theta_1(\eta x, p^2) \theta_4(\eta x, p^2) = C(p) \theta_1(\eta x, p)$, where $C[p]$ depends on p only.

2.2.5. *The Boltzmann weights.* Each set of four state-variables (h_1, h_2, h_3, h_4) at the corners of a face is assigned a weight $w(h_1, h_2, h_3, h_4 | u)$. There are six non-zero weights $w(h_1, h_2, h_3, h_4 | u)$, such that adjacent state-variables differ by ± 1 ,

³ Section 8.18 of [4]

⁴ We write the modular parameter of the nome p as $\tau' = 1/\tau$, instead of τ , for later convenience.

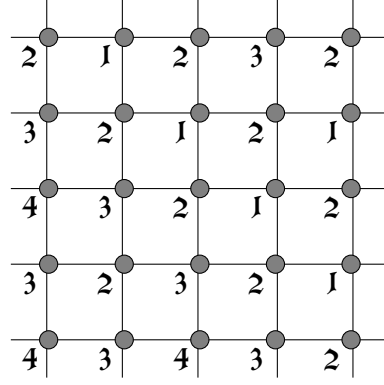


FIGURE 2.1. A configuration in the restricted solid-on-solid model $\mathcal{L}_{4,5}$, where the state-variables take values in $\{1, 2, 3, 4\}$.

$$(2.3) \quad w(h, h \pm 1, h \pm 2, h \pm 1 | u) = \frac{[u + 1]}{[1]},$$

$$(2.4) \quad w(h, h \pm 1, h, h \mp 1 | u) = \frac{[h \pm 1][u]}{[h][1]},$$

$$(2.5) \quad w(h, h \pm 1, h, h \pm 1 | u) = \frac{[h \mp u]}{[h]},$$

where u is a spectral parameter, and the bracket $[x]$ is defined in (2.2). All other weights are set to zero. The weights in (2.3–2.5) satisfy the interaction-round-a-face version of Yang-Baxter equations [3]. Depending on the choice of the remaining parameters, $\mathcal{L}_{m,m+1}$ can be in regime-I, -II, -III, or in regime-IV. We restrict our attention to regime-III, where $p, u \in \mathbb{R}$, and,

$$(2.6) \quad 0 < p < 1, \quad \text{and} \quad -1 < u < 0,$$

which guarantees that the Boltzmann weights are real. For a complete discussion of the restricted solid-on-solid models, we refer to [3].

2.2.6. *Remark.* The choice $-1 < u < 0$ in (2.6) makes the weights $w(h, h \pm 1, h, h \mp 1 | u)$ in (2.4) negative, but the signs of these weights can be changed without affecting the Yang-Baxter equations. This is because these weights appear either exactly once in each term in some Yang-Baxter equations, or an even number of times in each term in the remaining ones⁵.

2.2.7. *Remark.* From section 2.2.4, the Boltzmann weights in (2.3–2.5) could be written in the same form but in terms of the theta functions $\theta_1(x, p)$, as the factors $C(p)$ of section 2.2.4 cancel out. Both forms of the weights appear in the literature.

2.2.8. *Remark.* We use the notation $\mathcal{L}_{m,m+1}$ for the restricted solid-on-solid models considered in this work because these models flow at criticality to the unitary minimal conformal field theories $\mathcal{M}_{m,m+1}$ [5, 6], which form a subset of the minimal conformal field theories $\mathcal{M}_{m,m'}$, where m and m' are co-prime positive integers [7, 8].

2.3. Other restricted solid-on-solid models.

⁵ Equation (1.4.7) in [3]

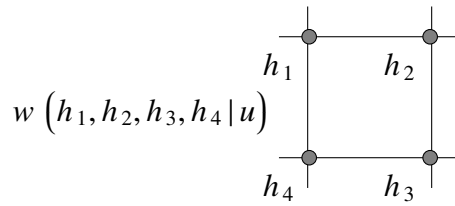


FIGURE 2.2. The weight $w(h_1, h_2, h_3, h_4 | u)$ associated to a face on the lattice with state-variables (h_1, h_2, h_3, h_4) at the corners, and a spectral parameter u .

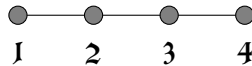


FIGURE 2.3. The Dynkin diagram A_4 that corresponds to the restricted solid-on-solid model $\mathcal{L}_{4,5}$, where the state-variables take values in $(1, 2, 3, 4)$.

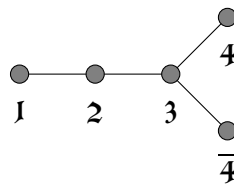


FIGURE 2.4. The Dynkin diagram D_5 that corresponds to the restricted solid-on-solid model $\mathcal{L}_{5,6}^D$, where the state-variables take values in $(1, 2, 3, 4, \bar{4})$.

2.3.1. *The Forrester-Baxter models.* The $\mathcal{L}_{m,m+1}$ models are obtained by setting the crossing parameter of the unrestricted solid-on-solid model $\eta = \pi / (m + 1)$. In [9], Forrester and Baxter set $\eta = n\pi / (m + 1)$, $n = 2, \dots, m$, and obtained a more general series of restricted solid-on-solid models that flow non-unitary minimal conformal field theories.

2.3.2. *Type-D restricted solid-on-solid models.* The off-critical solid-on-solid models of Andrews, Baxter and Forrester are related to A_m Lie algebras, starting from the fact that the allowed state-variables and their adjacencies correspond to the nodes of an A_m , $m = 3, 4, \dots$, Dynkin diagram, and the height state variables take values in $(1, 2, \dots, m)$. See Figure 2.3. It is common to refer to the models of Andrews *et al.* as type- A models. In [10], Pasquier introduced a class of off-critical solid-on-solid models whose allowed state-variables and their adjacencies correspond to the nodes of a D_m , $m = 4, 5 \dots$, Dynkin diagram, and the height state variables take values in $(1, \dots, m - 1, \overline{m - 1})$, and in [11, 12], solved these models and computed their local height probabilities. It is common to refer to the models of Pasquier as type- D models⁶.⁷ See Figure 2.4.

⁶ There are many more classes of generalized restricted solid-on-solid models, including the critical restricted solid-on-solid models based E_6 , E_7 and E_8 Dynkin diagrams, also due to Pasquier [10], but we do not need to recall these in the present work. For further references, we refer the reader to [13]

⁷ In another contribution [14], of relevance to the present work, Pasquier extended the Coulomb gas representation [15, 16] to the critical restricted solid-on-solid models.

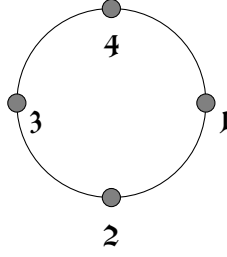


FIGURE 2.5. The Dynkin diagram of the affine Lie algebra \widehat{A}_4 that corresponds to the cyclic solid-on-solid model $\mathcal{L}_{4,5}^{\text{cyc}}$, where the state-variables take values in $(1, 2, 3, 4)$, and the height variables 1 and 4 are regarded as nearest-neighbours.

2.3.3. *The cyclic solid-on-solid models.* In [17, 18], Kuniba and Yajima studied cyclic solid-on-solid models where the height variables take values in the nodes of affine \widehat{A}_m Dynkin diagrams, see Figure 2.5, and used the corner transfer matrix method to compute their local height probabilities. In [17, 18], Kuniba and Yajima also study solid-on-solid models based on \widehat{D}_m Dynkin diagrams, but these results will not be referred to in the sequel. In [19, 20] studied the cyclic solid-on-solid models based on \widehat{A}_m Dynkin diagrams, in the presence of an extra parameter that acts as a simultaneous additive shift of the height variables.

3. FROM CORNER TRANSFER MATRICES TO LOCAL HEIGHT PROBABILITIES

We recall basic facts related to Baxter's corner transfer matrix method, and define the local height probabilities.

3.1. **The corner transfer matrix method.** The corner transfer matrix method originates in Baxter's work on the monomer-dimer problem [21], and was put in its current graphical form in [22]. For an introduction to the method, and an overview of its development, see [23, 24]. In [1, 2], Baxter used this method to compute the order parameters in the hard-hexagon model, and made an unexpected connection with the Rogers-Ramanujan identities [25]. This development led to the development of the restricted solid-on-solid models as an infinite series that includes the hard-hexagon model as a special case [3], and the corner transfer matrix method was used to compute the off-critical local height probabilities.

3.1.1. *Quadrants, boundaries, initial and final states.* Following [24, 3], we divide the square lattice into four quadrants, as in Figure 3.1. Each quadrant is bounded by an inner boundary, which is the vertex at the center of the lattice that carries a state-variable denoted by $a \in (1, \dots, m)$, an outer boundary that consists of a sequence of vertices such that adjacent vertices carry state-variables denoted by $(b, b \pm 1) \in (1, \dots, n)$, an initial half-line that one can regard as an initial state, and a final half-line that one can regard as a final state.

3.1.2. *Corner transfer matrices as operator.* A corner transfer matrix acts on the height variables on the initial half-line, and generates the height variables on the final half-line, such that the state-variables on the inner and outer boundaries are preserved. This action can be regarded as a transition from an initial to a final state, with a transition probability that can be computed in terms of the Boltzmann weights of the model. We denote the state-variables on the initial half-line and on the final half-line by,

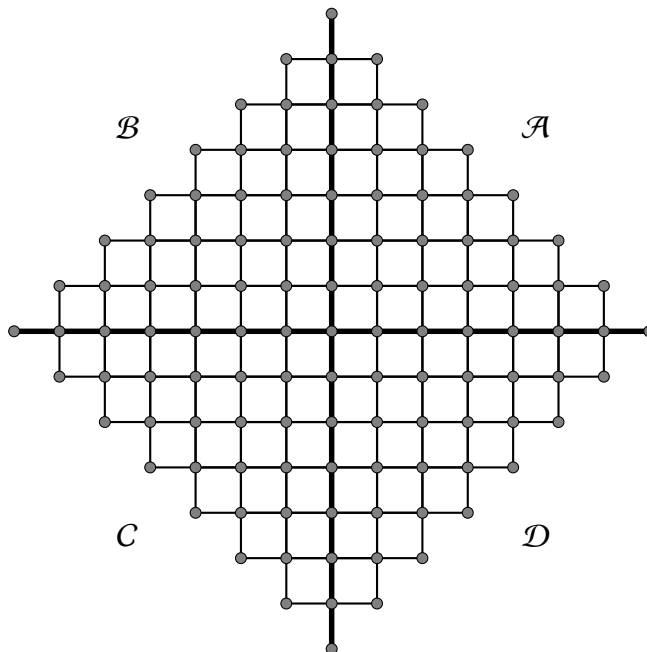


FIGURE 3.1. *The splitting of the lattice into four quadrants. We assume that the corner transfer matrices act counterclockwise. The corner transfer matrix \mathcal{A} acts on the horizontal line of vertices that extends from the center to the rightmost vertex, and generates the vertical line of vertices that extends from the center to the top site. This ‘transition’ is weighted by the partition function of this quadrant. \mathcal{B} , \mathcal{A} and \mathcal{D} act analogously.*

$$(3.1) \quad \mathbf{h} = (h_0, h_1, \dots, h_L, h_{L+1}), \quad \mathbf{h}' = (h'_0, h'_1, \dots, h'_L, h'_{L+1}),$$

respectively, where $h_0 = h'_0$ is the state-variable at the center of the lattice⁸. An element of the corner transfer matrix is the partition function of a quadrant, for fixed \mathbf{h} and \mathbf{h}' , that is, the sum over all allowed weighted configurations. The weight of an allowed configuration is the product of the weights of the faces of the configurations. We denote the corner transfer matrices of the four quadrants by \mathcal{A} , \mathcal{B} , \mathcal{C} , and \mathcal{D} . We refer to [24, 3] for the definition of the corner transfer matrix in terms of the Boltzmann weights.

3.1.3. *The partition function with fixed outer boundary conditions.* Let $\mathcal{L}_{m,m+1}$ be a regime-III restricted solid-on-solid model as in [3]. The off-critical partition function on a plane such that the state-variables on the outer boundary are fixed alternately at the ground-state pair $(b, b \pm 1)$ can be written in terms of corner transfer matrices as,

$$(3.2) \quad Z(b, b \pm 1 | p) = \text{Trace}(\mathcal{A}\mathcal{B}\mathcal{C}\mathcal{D})$$

where the trace over the product of corner transfer matrices in (3.2) indicates identifying the state-variables on the common half-diagonals, then summing over all state-variables that are not fixed by the outer boundary conditions, in all possible ways.

⁸ In [3], the state-variable at the center of the lattice is h_1 . In the present note, we use h_0 .

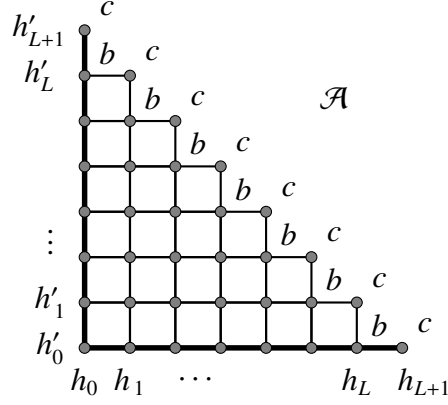


FIGURE 3.2. The \mathcal{A} quadrant, with state-variables h_i , $i = 0, 1, \dots, L + 1$, on the initial half-line/state, and h'_i , $i = 0, 1, \dots, L + 1$, on the final half-line/state, such that the state-variable on the inner boundary $h_0 = h'_0 = a$, and the state variables on the outer boundaries alternate as $(b, c = b \pm 1)$, and $a, b, c \in (1, 2, \dots, m)$.

3.2. The local height probabilities.

3.2.1. *Fixing the height at the inner boundary.* The partition function $Z(a, b, b \pm 1 | p)$ such that the state-variable h_0 , at the center of the lattice, is fixed, $h_0 = a$, and the state-variables on the outer boundary are fixed alternately at the ground-state pair $(b, b \pm 1)$, can be computed using corner transfer matrices by inserting the diagonal matrix \mathcal{S}_a , where,

$$(3.3) \quad (\mathcal{S}_a)_{\mathbf{h}, \mathbf{h}'} = \delta(h_0, a) \delta(\mathbf{h}, \mathbf{h}'), \quad \delta(\mathbf{h}, \mathbf{h}') \equiv \prod_{i=0}^{L+1} \delta(h_i, h'_i),$$

in (3.2), to obtain,

$$(3.4) \quad Z(a, b, b \pm 1 | p) = \text{Trace}(\mathcal{S}_a \mathcal{A} \mathcal{B} \mathcal{C} \mathcal{D}),$$

where $Z(a, b, b \pm 1 | p)$ is the two-dimensional configuration sum of the system with fixed boundary conditions both at the center and the boundary.

3.3. **Normalization to obtain probabilities.** The probability $P(a, b, b \pm 1 | p)$ that the height variable at the center of the lattice is a , while the state-variables on the boundary are $(b, b \pm 1)$, is obtained by normalizing $Z(a, b, b \pm 1 | p)$ by $\sum_{a'} Z(a', b, b \pm 1 | p)$, $a' = 1, \dots, m$, to obtain,

$$(3.5) \quad P(a, b, b \pm 1 | p) = \frac{\text{Trace}(\mathcal{S}_a \mathcal{A} \mathcal{B} \mathcal{C} \mathcal{D})}{\text{Trace}(\mathcal{A} \mathcal{B} \mathcal{C} \mathcal{D})}, \quad \sum_{a'} P(a', b, b \pm 1 | p) = 1,$$

and $P(a, b, b \pm 1 | p)$ is indeed a probability.

4. FROM LOCAL HEIGHT PROBABILITIES TO MODULAR FUNCTIONS

We outline the evaluation of the local height probabilities on a plane in six steps, in preparation for section 7, where these steps carry over with minimal modification to the $4N$ -quadrant case.

4.1. Evaluating the local height probabilities. In Appendix A of [3], Andrews *et al.* use the corner transfer matrix method to evaluate the off-critical local height probabilities, $P(a, b, b \pm 1 | p)$, in a planar geometry as functions of the Boltzmann weights, which in turn are functions of elliptic theta functions of nome p . They do this essentially as follows.

4.1.1. *Step 1. Factorize the corner transfer matrices.* The Yang-Baxter equations are used, in the thermodynamic limit, to factorize the corner transfer matrices in the form,

$$(4.1) \quad \mathcal{A}(u) = Q_1 M_1 e^{u\mathcal{H}} Q_2^{-1}, \quad \mathcal{B}(u) = Q_2 M_2 e^{-u\mathcal{H}} Q_3^{-1}, \\ C(u) = Q_3 M_3 e^{u\mathcal{H}} Q_4^{-1}, \quad \mathcal{D}(u) = Q_4 M_4 e^{-u\mathcal{H}} Q_1^{-1}$$

where the matrices $\mathcal{H}, M_1, \dots, M_4$, and Q_1, \dots, Q_4 are independent of the spectral parameter u . This is a major simplification, as the dependence of each corner transfer matrix on the spectral parameter u is now localized in an overall multiplicative factor in an exponent. The Yang-Baxter equations are also used to show that \mathcal{H} and M_1, \dots, M_4 are diagonal, which is another major simplification that allows us to use (4.1) in (3.5) to obtain,

$$(4.2) \quad P(a, b, b \pm 1 | p) = \frac{\text{Trace}(\mathcal{S}_a M_1 M_2 M_3 M_4)}{\text{Trace}(M_1 M_2 M_3 M_4)},$$

and find that $P(a, b, b \pm 1 | p)$ is independent of the spectral parameter u , which is a magnificent result, in the sense that it is enormously simpler than the expression that we started with.

4.1.2. *Step 2. Reduce the computation of $P(a, b, b \pm 1 | p)$ to a computation of \mathcal{H} .* To evaluate the matrix products in (4.2), Andrews *et al.* show that,

$$(4.3) \quad \mathcal{A}(\eta) = C(\eta) = \mathcal{I}, \quad \mathcal{B}(-\eta) = \mathcal{D}(-\eta) = \mathcal{R}_a,$$

where η is the crossing parameter, and \mathcal{R}_a is the diagonal matrix⁹,

$$(4.4) \quad (\mathcal{R}_a)_{h,h'} = [a]^{1/2} \delta(\mathbf{h}, \mathbf{h}'),$$

the bracket $[a]$ is defined in (2.2), and a is the fixed state-variable at the site at the centre of the lattice. From (4.1) and (4.3), and the fact that $Q_i, i = 1, \dots, 4$, and \mathcal{H} are diagonal, we obtain,

$$(4.5) \quad \mathcal{A}(\eta) \mathcal{B}(-\eta) C(\eta) \mathcal{D}(-\eta) = (\mathcal{R}_a)^2, \quad M_1 M_2 M_3 M_4 = (\mathcal{R}_a)^2 e^{-4\eta\mathcal{H}},$$

so that,

⁹ \mathcal{R}_a in this work is \mathcal{R}_1 in [3].

$$(4.6) \quad P(a, b, b \pm 1 | p) = \frac{\text{Trace} \left(\mathcal{S}_a \left(\mathcal{R}_a \right)^2 e^{-4\eta\mathcal{H}} \right)}{\text{Trace} \left(\left(\mathcal{R}_a \right)^2 e^{-4\eta\mathcal{H}} \right)},$$

and the computation of the complicated $P(a, b, b \pm 1 | p)$ is reduced to that of the much simpler \mathcal{H} .

4.1.3. *Step 3. Show that the elements of \mathcal{H} are integer multiples of $2\pi/\tau$.* Setting $u = \eta$ in the first equation in (4.1), and using the first equation in (4.3), it is clear that,

$$(4.7) \quad \mathcal{Q}_1 \mathcal{M}_1 = \mathcal{Q}_2 e^{-\eta\mathcal{H}},$$

from which it follows that,

$$(4.8) \quad \mathcal{A}(u) = \mathcal{Q}_2 e^{(u-\eta)\mathcal{H}} \mathcal{Q}_2^{-1}$$

Since $\mathcal{A}(u)$ is a function of elliptic theta functions of nome $p = e^{-2\pi/\tau}$, the exponential $e^{(u-\eta)\mathcal{H}}$ can be calculated using the quasi-periodicity properties of $\mathcal{A}(u)$, and the elements of \mathcal{H} must be integer multiples of $2\pi/\tau$. These integers can be computed by taking a suitable limit.

4.1.4. *Remark.* The fact that (the essential factor, that carries the statistical mechanical information) in the corner transfer matrix is an exponential, as in (4.8), is arguably the most important property of the corner transfer matrix, and the one that underlies the result in this work.

4.1.5. *Step 4. Perform a conjugate modulus transformation.* To take the limit that allows one to compute the elements of \mathcal{H} , Andrews *et al.* perform a conjugate modulus transformation that replaces the nome p of the theta functions that appear in the weights with a conjugate nome q such that,

$$(4.9) \quad p = e^{-2\pi/\tau}, \quad q = e^{-4\pi\tau/(m+1)}, \quad \tau \in \mathbb{R}$$

4.1.6. *Step 5. Compute \mathcal{H} in unevaluated form.* Working in terms of elliptic theta functions with conjugate nome q , Andrews *et al.* found that $e^{-4\eta\mathcal{H}}$ takes the form,

$$(4.10) \quad \left(e^{-4\eta\mathcal{H}} \right)_{\mathbf{h}, \mathbf{h}'} = q^{(\Phi(\mathbf{h}) - (2a-m-1)^2/16(m+1))} \delta(\mathbf{h}, \mathbf{h}'),$$

where $\Phi(\mathbf{h})$ is the $L \rightarrow \infty$ limit of the corner transfer matrix energy function $\Phi_L(h_0, \dots, h_{L+1})$,

$$(4.11) \quad \Phi_L(h_0, \dots, h_{L+1}) = \sum_{j=1}^L j \mathcal{H}(h_{j-1}, h_j, h_{j+1}), \quad \mathcal{H}(h_{j-1}, h_j, h_{j+1}) = \frac{1}{4} |h_{j-1} - h_{j+1}|$$

Writing $(\mathcal{R}_a)_{\mathbf{h}, \mathbf{h}'}$ in terms of q ,

$$(4.12) \quad (\mathcal{R}_a)_{\mathbf{h}, \mathbf{h}'} = \tau q^{(h_0 - m - 1)^2 / 8(m+1)} E(q^{a/2}, q) \delta(\mathbf{h}, \mathbf{h}'),$$

$$E(z, q) = \prod_{n=1}^{\infty} (1 - q^{n-1}z) (1 - q^{n-1}z^{-1}) (1 - q^n),$$

Andrews *et al.* obtain the local height probability in terms of q ,

$$(4.13) \quad P(a, b, b \pm 1 | q) = \frac{E(q^{a/2}, q^{(m+1)/2}) X(a, b, b \pm 1 | q)}{\sum_{1 \leq a' < m} E(q^{a'/2}, q^{(m+1)/2}) X(a', b, b \pm 1 | q)},$$

where X is a one-dimensional configuration sum defined as ¹⁰,

$$(4.14) \quad X(a, b, b \pm 1 | q) = \lim_{L \pi_{ab} \rightarrow \infty} X_L(a, b, b \pm 1 | q),$$

π_{ab} is the parity of $|a - b|$, and the finite-length one-dimensional sum $X_L(a, b, b \pm 1 | q)$ is,

$$(4.15) \quad X_L(a, b, b \pm 1 | q) = \sum_{(h_1, \dots, h_{L-1}) \in (1, \dots, m)} q^{\Phi_n(h_0, \dots, h_{L+1})}, \quad h_i - h_{i+1} = \pm 1,$$

with the boundary state-variables fixed at $h_0 = a, h_L = b, h_{L+1} = b \pm 1$. The limit in (4.14) is taken over all even values L_{even} , or odd values L_{odd} of L , depending on the parity π_{ab} of $|a - b|$. The one-dimensional configuration sum $X(a, b, b \pm 1 | q)$, encodes the statistical mechanics of the model.

4.1.7. *Remark.* Aside from a boundary factor that depends only on the state-variable a at the center of the lattice, all information about the statistical mechanics of $P(a, b, b \pm 1 | q)$ is encoded in the one-dimensional configuration sum $X(a, b, b \pm 1 | q)$, which is a q -series in the conjugate nome q , that encodes the multiplicities and energy-levels of the states that contribute to $P(a, b, b \pm 1 | q)$.

4.1.8. *Step 6. Evaluate the one-dimensional configuration sums.* Andrews *et al.* evaluate the one-dimensional configuration sums $X(a, b, b \pm 1 | q)$ by solving the recurrence relations that determine them completely, subject to the initial conditions that they satisfy. They obtain the solution in the form of an alternating-sign q -series ¹¹,

$$(4.16) \quad X(a, b, b \pm 1 | q) = \frac{q^{\frac{1}{4}b(b \pm 1)}}{\eta(q)} \Delta\left(a, \frac{1}{2}(b + (b \pm 1) - 1) | q\right), \quad \eta(q) = \prod_{n=1}^{\infty} (1 - q^n),$$

$$\Delta(\alpha, \beta | q) = \sum_{n \in \mathbb{Z}} q^{m(m+1)n^2 + \beta(m+1)n + \frac{1}{4}\alpha(\alpha-1)} \left(q^{-\alpha mn - \frac{1}{2}\alpha\beta} - q^{\alpha mn + \frac{1}{2}\alpha\beta} \right)$$

4.2. Modular functions.

¹⁰ We choose to make the dependence on q explicit, as this will change in the sequel.

¹¹ These alternating q -series are also known as the Rocha-Caridi Virasoro characters [26]

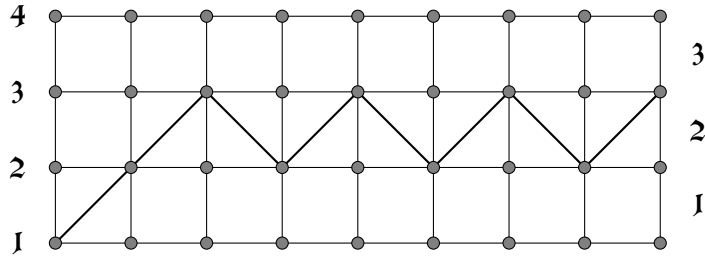


FIGURE 4.1. A minimal path in the restricted solid-on-solid model $\mathcal{L}_{4,5}$, and this particular path belongs to the one-dimensional configuration sum labeled by $a = 1$, $b = 2$, and $c = 3$. The numbers on the left label the possible initial points of paths, and correspond to the label s in $\chi_{r,s}^{Vir}$. The numbers on the right label the possible final bands that paths can end up oscillating in, and correspond to the label r in $\chi_{r,s}^{Vir}$.

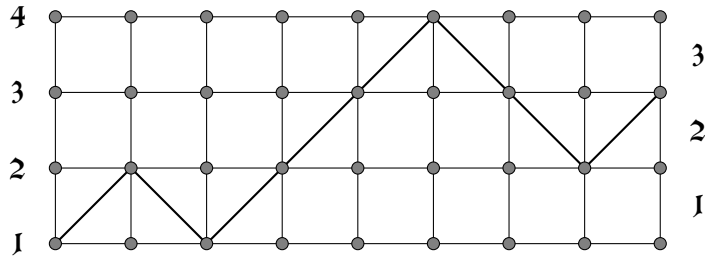


FIGURE 4.2. A non-minimal path in the restricted solid-on-solid model $\mathcal{L}_{4,5}$, that belongs to the one-dimensional configuration sum labeled by $a = 1$, $b = 2$, and $c = 3$.

4.2.1. *The one-dimensional configurations sums are modular functions.* The q -series $\Delta(\alpha, \beta | q)$ in (4.16) is essentially the difference of two theta functions, and the result of the evaluation is that the one-dimensional configuration sums are modular functions. In the case of the hard-hexagon model, q -series identities due to Schur relate these modular functions to q -series with non-negative coefficients that appear as sum-sides of Rogers-Ramanujan identities [2, 25]¹².

4.2.2. *Remark. Paths.* The one-dimensional configuration sums are partition functions of paths on a Dynkin diagram that can be represented as paths on lattice as in Figures 4.1, and 4.2. The path in Figure 4.1 belongs to a configuration sum labelled by $a = 1$, $b = 2$, and $c = 3$. It is a minimal path in the sense that it starts from $a = 1$, and reaches $b = 2$, to oscillate in the band $(b, c) = (2, 3)$, in a minimal number of steps. The path in Figure 4.2 belongs to the same configuration sum labelled by $a = 1$, $b = 2$, and $c = 3$, as in Figure 4.1, but is non-minimal in the sense that it starts from $a = 1$, and reaches $b = 2$, to oscillate in the band $(b, c) = (2, 3)$, in a non-minimal number of steps. Computing the energy of a path using (4.15), the minimal path in a particular one-dimensional configuration sum has a lower energy than any other path.

¹² This observation led Andrews, Baxter and Forrester to develop the restricted solid-on-solid models as extensions of the hard-square version of the hard-hexagon model, and also led Date, Jimbo, Miwa and Okado to their work on the connection between off-critical one-dimensional sums and Virasoro characters as discussed in section 5

4.2.3. *Remark. q -Series representations of the one-dimensional configuration sums with positive-definite coefficients.* Following the work of Kedem, Klassen, McCoy and Melzer [27, 28] on the positive-definite representations of the Virasoro characters, extensive studies of the path representations of the one-dimensional configuration sums, including [29–36] and references therein, led to evaluations of large classes of Virasoro characters in terms of q -series with positive-definite coefficients.

5. OFF-CRITICAL LOCAL HEIGHT PROBABILITIES IN A PLANAR GEOMETRY ARE AFFINE AND VIRASORO CHARACTERS

We recall the definitions of affine and Virasoro characters, then following [37], we write the local height probabilities in terms of characters.

5.1. Affine characters.

5.1.1. *Theta functions with characteristics.* Following [38], the characteristic- i , level- j theta function is,

$$(5.1) \quad \theta_{i,j}(z, q) = \sum_{n \in \mathbb{Z}} q^{j \left(n + \frac{i}{2j}\right)^2} z^{j \left(n + \frac{i}{2j}\right)},$$

where $i \in (0, 1, \dots, j)$, $j \in (1, 2, \dots)$, q is the nome parameter, and $z \in \mathbb{C}$.

5.1.2. *A linear combination of theta functions with characteristics.* Following [39], we define the linear combination of theta functions with characteristics¹³,

$$(5.2) \quad \Theta_{i,j}(z, q) = \sum_{n \in \mathbb{Z}} q^{j \left(n + \frac{i}{2j}\right)^2} \left(z^{-j \left(n + \frac{i}{2j}\right)} - z^{j \left(n + \frac{i}{2j}\right)} \right)$$

5.1.3. *Affine characters.* Following Kac and Peterson [39], the character of the charge- i , level- j $\mathcal{U}_q(\widehat{sl}_2)$ irreducible highest-weight module can be written in terms of theta functions as¹⁴,

$$(5.3) \quad \widehat{\chi}_{i,j}(z, q) = \frac{\Theta_{i+1, j+2}(z, q)}{\Theta_{1,2}(z, q)},$$

where $\Theta_{i+1, j+2}(z, q)$ is defined in (5.2).

5.2. Virasoro characters.

¹³ This is the second equation in (7), in [37], with appropriate changes in notation.

¹⁴ First equation in (7), in [37], with appropriate changes in notation. Note the shift in the indices of the theta function in the numerator of the right hand side with respect to those of the affine character on the left hand side.

5.2.1. *Virasoro characters as branching functions.* Based on the work of Kac and Peterson [39], on affine Lie algebras and theta functions, Date, Jimbo, Miwa, and Okado show, in [37], that the product of two affine characters decomposes in the form,

$$(5.4) \quad \widehat{\chi}_{j_1, m-2}(z, q) \widehat{\chi}_{j_2, 1}(z, q) = \sum_{j_3} c_{j_1 j_2 j_3}(q) \widehat{\chi}_{j_3, m-1}(z, q),$$

where the branching coefficients $c_{j_1 j_2 j_3}(q)$ are characters of the fully-degenerate irreducible Virasoro highest-weight modules that appear in the unitary rational conformal field theories of Friedan, Qiu and Shenker [5, 6]¹⁵, in parallel with the coset construction of these Virasoro modules in terms of $\mathcal{U}_q(\widehat{sl}_2)$ highest-weight modules by Goddard, Kent and Olive [41, 42].

5.2.2. *Notation.* The notation $c_{j_1 j_2 j_3}(q)$ used for the branching coefficients of products of affine characters in (5.4), which are Virasoro characters, is related to the notation $\chi_{r,s}^{Vir}(q)$ that is currently more commonly used for Virasoro characters, as follows. For $c = b + 1$,

$$(5.5) \quad c_{j_1 j_2 j_3}(q) = c_{b, 1, a}(q) = \chi_{b, a}^{Vir}(q),$$

and for $c = b - 1$,

$$(5.6) \quad c_{j_1 j_2 j_3}(q) = c_{c, 2, a}(q) = \chi_{c, a}^{Vir}(q)$$

In other words, the first index j_1 in $c_{j_1 j_2 j_3}$ is equal to the first index r in $\chi_{r,s}^{Vir}$, and takes the value of the smaller of the outer boundary state-variables (b, c) , the second index j_2 in $c_{j_1 j_2 j_3}$ is either 1 or 2 depending on whether $c = b + 1$ or $b - 1$, respectively, and the third index j_3 in $c_{j_1 j_2 j_3}$ is equal to the second index s in $\chi_{r,s}^{Vir}$, and takes the value of the inner boundary state-variable a .

5.2.3. *One-dimensional configuration sums are Virasoro characters.* In [37, 40], Date, Jimbo, Miwa and Okado observe that the regime-III one-dimensional sum $X(a, b, b \pm 1 | q)$ is identical to the character of a Virasoro highest-weight module in a unitary minimal conformal field theory, up to a q -factor¹⁶,

$$(5.7) \quad X(a, b, b \pm 1 | q) = q^\nu c_{j_1 j_2 j_3}(q),$$

where,

$$(5.8) \quad \nu = \frac{1}{4} \left[(b-a) - \frac{j_1^2}{m} - \frac{j_2^2}{3} + \frac{j_3^2}{(m+1)} + \frac{1}{2} \right],$$

$$j_1 = \left(\frac{b+c}{2} \right) - \frac{1}{2}, \quad j_2 = \left(\frac{b-c}{2} \right) + \frac{3}{2}, \quad j_3 = a$$

¹⁵ Note that the level indices of the affine characters are such that, for $m = 3$, we get the Virasoro characters of the coset model that corresponds to the Ising model.

¹⁶ Further details with full proofs can be in the work of Date *et al.* with Kuniba [43, 44],

The branching coefficients c_{j, j_2, j_3} in (5.4) are characters of the Virasoro highest-weight modules that appear in the unitary minimal conformal field theories $\mathcal{M}_{m, m+1}$ of Friedan, Qiu and Shenker [5, 6]. $\mathcal{M}_{m, m+1}$ were identified by Huse [45] as the *critical* limit of the $\mathcal{L}_{m, m+1}$ solid-on-solid models [3], that we are interested in in this work. The affine characters $\widehat{\chi}_{i, j}$ in (5.4) are characters of the \widehat{sl}_2 Wess-Zumino-Witten models used by Goddard, Kent and Olive [41, 42] to construct $\mathcal{M}_{m, m+1}$.

5.3. Re-writing the local height probabilities in terms of affine and Virasoro characters. Following [37], we use the identity¹⁷,

$$(5.9) \quad E(q^{i/2}, q^{j/2}) = q^{\frac{i(j-i)}{4j}} \Theta_{i, j}(q^{\frac{1}{2}}, q),$$

as well as (5.3–5.4), to rewrite (4.13) in terms of theta functions and Virasoro characters,

$$(5.10) \quad P(a, b, b \pm 1 | q) = \left(q^{-y} \frac{\Theta_{j_3+1, m+1}(q^{1/2}, q) \Theta_{1, 2}(q^{1/2}, q)}{\Theta_{j_1+1, 3}(q^{1/2}, q) \Theta_{j_2+1, m}(q^{1/2}, q)} \right) (q^y c_{j_1, j_2, j_3}(q)),$$

where (j_1, j_2, j_3) are related to $(a, b, c = b \pm 1)$ as in (5.5–5.6), and the $q^{\pm y}$ -factors are positioned to make the origin of the various factors clear.

6. CRITICAL PARTITION FUNCTIONS IN A CYLINDRICAL GEOMETRY

We recall basic works related to our understanding of the critical partition functions in a cylindrical geometry as Virasoro characters.

6.1. Numerical results. In [46], Gehlen and Rittenberg study the spectra of the quantum Hamiltonians of the Ising (2-state Potts) and the 3-state Potts spin-chains on a finite-height, infinite-circumference cylindrical-geometry, with free boundary conditions in the finite-height direction¹⁸. In the Ising case, they use the exact diagonalization of the Ising quantum Hamiltonian of [47, 48], and in the 3-state Potts case, they diagonalize the quantum Hamiltonian numerically. In both cases, they show that the scaling operators fall into fully-degenerate irreducible Virasoro highest-weight modules of a single Virasoro algebra, as opposed to the direct product of two commuting Virasoro algebras as in the same models on a domain with periodic boundary conditions [49], and the corresponding partition functions of these models with these boundary conditions are linear (as opposed to bilinear) sums of characters of these modules¹⁹.

6.2. Analytic results. In [51], Cardy used the inversion sum rules, that follow from requiring consistency under modular transformations, to study the spectra of the transfer matrices of the unitary minimal Virasoro conformal field theories of Friedan, Qiu and Shenker [5, 6], in the same finite-height, infinite-circumference cylindrical-geometry of [46], with **1.** free boundary conditions as in [46], **2.** fixed boundary conditions (the order parameter is fixed to the same

¹⁷ Equation (2.13) in [43], with $x^2 \rightarrow q$, $j \rightarrow i$, $m \rightarrow j$, $\epsilon_1 = -$, $\epsilon_2 = +$, dropping the superscripts off Θ in (2.13), and re-arranging terms.

¹⁸ In [46], this geometry is referred to as a strip geometry with a finite-direction and an infinite-direction, and periodic boundary conditions in the latter direction.

¹⁹ That one Virasoro algebra (as opposed to two commuting Virasoro algebras) is needed in the presence of a boundary was expected on the basis of analogous computations in open (as opposed to closed) string theories [50]

value on both boundaries, or two different values on the two boundaries), and **3.** mixed boundary conditions (fixed boundary conditions on one boundary and free boundary conditions on the other), in the finite-direction. Cardy obtained complete analytic results for the partition functions of these models, with these boundary conditions, as linear sums of the full-degenerate irreducible Virasoro highest-weight modules of a single Virasoro character, in agreement with, and extension of [46].

6.3. Solid-on-solid and restricted-solid-on-solid results. In [52], Saleur computed the partition function of the solid-on-solid version of the six-vertex model on a cylinder with the bottom-row of state-variables fixed at $a \in \mathbb{Z}$, and the top-row of state-variables fixed at $c \in \mathbb{Z}$, for admissible choices of a and c . In [53], Saleur and Bauer extended the results in [52] to two classes of models on a cylinder of dimensions $H \times W$, where W is the circumference of the periodic direction, with more general boundary conditions in the non-periodic direction of length H , namely **1.** the critical solid-on-solid version of the six-vertex model on a cylinder with boundary conditions such that the bottom-row of state-variables is fixed at height $a \in \mathbb{Z}$, the second-from-top-row of state-variables is fixed at height $b \in \mathbb{Z}$, and the top-row of state-variables is fixed at height $c \in \mathbb{Z}$, $b - c = \pm 1$, with admissible choices of a, b and c , given the number of rows H in the non-periodic direction of the cylinder, and **2.** the critical version of the restricted solid-on-solid models of Andrews, Baxter and Forrester [3], and the critical solid-on-solid models of Pasquier [10], on a cylinder with boundary conditions as in **1**, but with the state-variables a, b and c suitably restricted.

6.3.1. The Bethe Ansatz. Because the boundary conditions in [53] are more elaborate than those in [52], Saleur and Bauer use, not only the Coulomb gas representation of restricted solid-on-solid models [11], but also the Bethe Ansatz analysis of [54, 55]. They find that the critical partition functions of the models that they consider on a cylinder are Virasoro characters labelled by a, b and $c = b \pm 1$.

6.3.2. Relation to the work of Date et al. Saleur and Bauer find that the spectrum of the *off-critical* regime-III corner transfer matrix Hamiltonian is, up to a shift in the ground state eigenvalue, the same as the spectrum of the corresponding *critical* continuum-limit Hamiltonian on a cylinder, for the same fixed boundary conditions, *if* the deviation from criticality in the former model is identified with the finite-size L of the non-periodic direction of the cylinder in the latter²⁰. Recalling the result of Date *et al.* [37, 40], Saleur and Bauer found concrete examples to the effect that off-critical local height probabilities, in type-*A* and type-*D* regime-III restricted solid-on-solid models on a plane, are essentially the same objects as the partition functions of critical conformal field theories on a cylinder, for matching choices of boundary state-variables a, b and c , and a suitable mapping of the the role of departure from criticality in the off-critical problem on a plane to the finite-size in the critical problem on a cylinder.

The present work motivates why the aspect-ratio of the annular, or equivalently cylinder geometry of the critical conformal field theories can be identified with the distance from criticality in the corresponding off-critical statistical mechanical models.

²⁰ In [53], Saleur and Bauer also study critical and tri-critical Potts model partition functions on a cylinder and obtain results in the form of linear combinations of Virasoro characters in agreement with, and extension of Gehlen and Rittenberg's numerical results [46], and Cardy's analytic results [51]. Please note that reference [14] in [53] is incorrect, and should be replaced with reference [51] in the present work.

6.4. Restricted-solid-on-solid models on a spiral geometry. The main idea in the present work is **1.** to extend the definition of the local height probability $P(a, b, b \pm 1 | p)$ from the 4-quadrant planar geometry to a $4N$ -quadrant spiral geometry, where $N = \frac{5}{4}, \frac{6}{4}, \dots$, and at the same time **2.** allow the modular parameter τ , whose inverse $\tau' = \frac{1}{\tau}$ measures departure from criticality, to depend on N , and write the new N -dependent modular parameter as τ_N . This way, we obtain an object that interpolates the off-critical local height probabilities on a plane and the critical partition functions on a cylinder.

7. EVALUATING LOCAL HEIGHT PROBABILITIES IN A SPIRAL GEOMETRY

We repeat the derivation in section 4.1 of the off-critical local height probabilities, but now in a spiral geometry. We show that all steps carry through with minimal modification.

7.1. From an off-critical system on a plane to a near-critical system on a ‘deep’ spiral.

We show that the computation of the local height probabilities of Andrews *et al.* extends to a $4N$ -quadrant geometry without obstruction. Starting from an off-critical system with weights in terms of elliptic theta functions, with a modular parameter τ , and increasing the number of quadrants to $4N$, then aside from factors that do not carry information about the statistical mechanics of the local height probabilities, we essentially only change the modular parameter from τ to $\tau_N = \tau/N$. In other words, we find that the essential factor in the local height probability, evaluated on a $4N$ -quadrant geometry, which is the one-dimensional configuration sum, becomes $X(a, b, b \pm 1 | q^N)$, where $q = e^{-4\pi\tau/(m+1)}$. Now if we also vary τ , make that τ_N , and choose $\tau_N = \tau/N$, then the one-dimensional configuration sums remain invariant. This means that, apart from overall factors that are blind to the statistical mechanics, the off-critical local height probability on a plane is equal to that on a spiral with $4N$ -quadrants. For sufficiently-large but finite N , the spiral is ‘deep’, in the sense that it has many quadrants, that is a large number of turns, but still finite, and the model that lives on it is near-criticality, in the sense that the nome p of the elliptic theta functions in which the Boltzmann weights are expressed, is finite but small.

7.2. $4N$ -quadrant geometry. Following [24], Chapter 13, we consider a finite version of a square lattice as in Figure 1. We take N copies of the above finite lattice, labelled by $i \in (1, 2, \dots, N)$ and *cut* each copy along a half-line that extends from the center of the lattice to a corner, *e.g.* the East corner. This splits each site on the cut half-line into two. We denote the upper and lower split half-lines by h_{i+} and h_{i-} , respectively. We identify h_{i+} and $h_{(i+1)-}$ for $i \in (1, 2, \dots, N-1)$ and identify h_{i+} to $h_{(i+1)-}$ to obtain a $4N$ -quadrant spiral geometry with periodic boundary conditions in the angular direction.

7.3. Local height probabilities on $4N$ -quadrants. Our task is identical to that in section 4.1, on a $4N$ -quadrant lattice, $N \in \mathbb{N} > 1$, rather than $N = 1$, so that now we have N copies of each quadrant, $\mathcal{A}_i(v)$, *etc.*

7.3.1. Step 1 on a spiral. Using the Yang-Baxter equations, we obtain,

$$(7.1) \quad \begin{aligned} \mathcal{A}_i(u) &= Q_{1,i} M_{1,i} e^{u\mathcal{H}} Q_{2,i}^{-1}, & \mathcal{B}_i(u) &= Q_{2,i} M_{2,i} e^{-u\mathcal{H}} Q_{3,i}^{-1}, \\ C_i(u) &= Q_{3,i} M_{3,i} e^{u\mathcal{H}} Q_{4,i}^{-1}, & \mathcal{D}_i(u) &= Q_{4,i} M_{4,i} e^{-u\mathcal{H}} Q_{1,i}^{-1} \end{aligned}$$

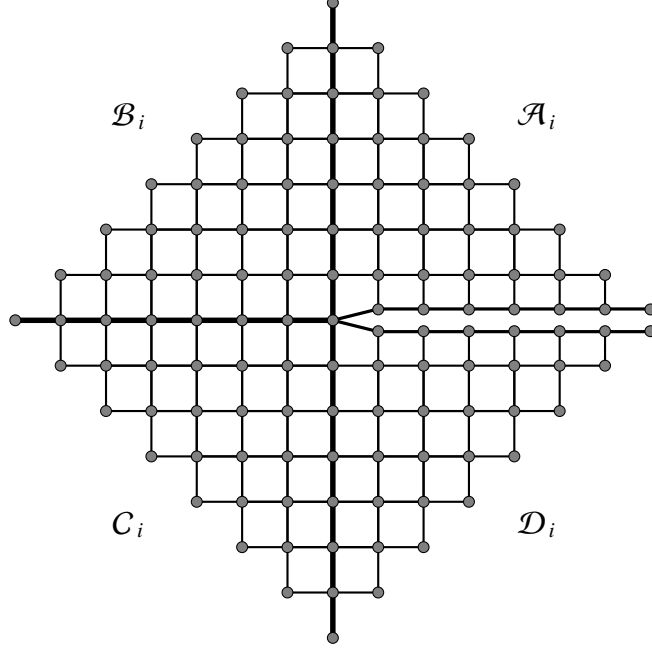


FIGURE 7.1. We cut the 4-quadrant lattice along a half-line, then prepare N copies of the cut lattices, labeled by $i \in 1, 2, \dots, N$.

where \mathcal{H} is the same, and the matrices \mathcal{M}_i and \mathcal{Q}_i , $i = 1, \dots, N$, have the same properties as on a plane. This allows us to write,

$$(7.2) \quad P_N(a, b, b \pm 1 | p_N) = \frac{\text{Trace} (S_a M_{1,1} M_{2,1} M_{3,1} \cdots M_{3,N} M_{4,N} M_{1,N})}{\text{Trace} (M_{1,1} M_{2,1} M_{3,1} \cdots M_{3,N} M_{4,N} M_{1,N})},$$

where $P_N(a, b, b \pm 1 | p_N)$ is the local height probability on a spiral geometry with $4N$ quadrants, that is winding number N , the notation p_N indicates that we allow the nome p to vary with N , and we take $P_1(a, b, b \pm 1 | p_1) = P(a, b, b \pm 1 | p)$.

7.3.2. *Step 2 on a spiral.* The analysis of each separate quadrant is independent of the total number of quadrants, and in particular, for $N > 1$, the relations,

$$(7.3) \quad A_i(\eta) = C_i(\eta) = I, \quad C_i(-\eta) = D_i(-\eta) = R_a,$$

still apply, where η is the crossing parameter, and R_a is the diagonal matrix with entries,

$$(7.4) \quad (R_a)_{h,h'} = [a]^{1/2} \delta(\mathbf{h}, \mathbf{h}'),$$

and a is the fixed height at the site at the centre of the lattice. Following section 4.1, we write,

$$(7.5) \quad \prod_i A_i(\eta) B_i(-\eta) C_i(\eta) D_i(-\eta) = R_a^{2N}, \quad M_{1,1} M_{2,1} \cdots M_{3,N} M_{4,N} = R_a^{2N} e^{-4N\eta\mathcal{H}},$$

and we obtain,

$$(7.6) \quad P_N(a, b, b \pm 1 | p_N) = \frac{\text{Trace} \left(S_a R_a^{2N} e^{-4N\eta\mathcal{H}} \right)}{\text{Trace} \left(R_a^{2N} e^{-4N\eta\mathcal{H}} \right)}$$

7.3.3. *Step 3 and Step 4 on a spiral.* These two steps carry through without modification from a plane to a deep spiral.

7.3.4. *Step 5 on a spiral.* Working in terms of elliptic theta functions with a conjugate nome q_N , that depends on the winding number N , the arguments of Andrews *et al.* carry through with minimal modification and we obtain,

$$(7.7) \quad \left(e^{-4N\eta\mathcal{H}} \right)_{h, h'} = q_N^{N(\Phi(h) - (2a-m-1)^2/16(m+1))} \delta(\mathbf{h}, \mathbf{h}'),$$

where Φ is the same $L \rightarrow \infty$ limit of the corner transfer matrix energy function Φ_n in (4.11), and we also obtain,

$$(7.8) \quad (R_a)_{h, h'} = \tau^N q_N^{N(a-m-1)^2/8(m+1)} E^N(q_N^{a/2}, y) \delta(\mathbf{h}, \mathbf{h}')$$

Using these results,

$$(7.9) \quad P_N(a, b, b \pm 1 | q_N) = \frac{E^N(q_N^{a/2}, q_N^{(m+1)/2}) X(a, b, b \pm 1 | q_N^N)}{\sum_{1 \leq a' < r} E^N(q_N^{a'/2}, q_N^{(m+1)/2}) X(a', b, b \pm 1 | q_N^N)},$$

where the one-dimensional configuration sum $X(a, b, b \pm 1 | q_N^N)$ is a q_N^N -series.

7.3.5. *Remark.* It is crucial to note that the one and only effect of the winding number N on the essential factor in the corner transfer matrix computation of the local height probability is the factor N in the exponential in (7.7), and that this factor simply modifies the modular parameter as $\tau_N \rightarrow N\tau_N$. This is the essential observation in this work.

7.3.6. *Step 6 on a spiral.* The one-dimensional configuration sum $X(a, b, b \pm 1 | q_N^N)$ satisfies the same difference equations, and the same initial conditions as $X(a, b, b \pm 1 | q)$, and can be evaluated similarly. The result is proportional to the same Virasoro character as before, but with $q \rightarrow q_N^N$.

7.4. **Scaling L and τ with N .** In the sequel, as we vary the number of quadrants $4N$, we need to scale L , the number of sites in a one-dimensional configuration, which is basically a measure of the radial extension of the lattice, and τ , which is a measure of departure from criticality, as functions of N . We call the scaled parameters L_N and τ_N , and choose them as,

$$(7.10) \quad L_N = (NL)^N, \quad \tau_N = \tau / N,$$

where $L = L_1$ and $\tau = \tau_1$, the parameters that we start from on a plane.

7.4.1. *Remark.* We interpret the multiplicative factor N in $(NL)^N$ as a filling in of the lattice with more vertices, so that the limit $N \rightarrow \infty$, can be interpreted as a thermodynamic limit, and at criticality, we end up with a system of finite size $(L')^N$, where L' is a finite length of a system with continuous degrees of freedom. The power N further increases the size of the lattice, but will be undone as we conformally transform the spiral geometry to an annular geometry.

7.5. **A change of normalization.** Consider (7.9). Since we wish to compute critical partition functions, rather than local height probabilities, we are allowed to choose convenient normalization such that the quantities that we are computing do not necessary add up to 1, as probabilities do. We need to choose a normalization that agrees with (4.13) at $N = 1$, but is allowed to be different for $N \neq 1$. We consider the quantity,

$$(7.11) \quad P'_N(a, b, b \pm 1 | q_N) = \frac{E^N \left(q_N^{a/2}, q_N^{(m+1)/2} \right) X(a, b, b \pm 1 | q_N^N)}{\sum_{1 \leq a' < r} \left(E \left(q_N^{a'/2}, q_N^{(m+1)/2} \right) X(a', b, b \pm 1 | q_N^N) \right)^N}$$

We need this modified normalization to make contact with the results of [53]. Notice that the new normalization differs from the original by an overall factor that does not change the relative weights of the configurations.

7.6. **Writing the local height probabilities on a spiral in terms of affine and Virasoro characters.** On a spiral, (5.10) becomes,

$$(7.12) \quad P_N(a, b, b \pm 1 | q_N) = \left(\frac{\Theta_{j_3, m-1}(q_N^{1/2}, q_N) \Theta_{1,2}(q_N^{1/2}, q_N)}{\Theta_{j_1, m}(q_N^{1/2}, q_N) \Theta_{j_3, 3}(q_N^{1/2}, q_N)} q_N^{-\nu} \right)^N (q_N^{N\nu} c_{j_1 j_2 j_3}(q_N^N)) \\ = \left(\frac{\Theta_{j_1, m-1}(q_N^{1/2}, q_N) \Theta_{1,2}(q_N^{1/2}, q_N)}{\Theta_{j_2, m}(q_N^{1/2}, q_N) \Theta_{j_2, 3}(q_N^{1/2}, q_N)} \right)^N c_{j_1 j_2 j_3}(q_N^N),$$

where the parameters a, b , and $b \pm 1$ on the left are related to the parameters j_1, j_2 , and j_3 on the right as in (5.5–5.6). Finally, we formally take $N \in \mathbb{R}$. Equation (7.12), with $N \in \mathbb{R}$, is the result that we need.

8. CRITICAL PARTITION FUNCTIONS ON A CYLINDRICAL GEOMETRY REVISITED

8.1. **Two regularizations before taking the infinite-spiral limit.** To take the $N \rightarrow \infty$ of a critical theory on an infinite-spiral, and more importantly, to conformally transform the spiral to an annulus with a finite aspect-ratio that can be conformally transformed to a cylinder, so that we end up with a critical model on a cylinder, we need two regularizations.

8.1.1. *Regularization 1. Infrared.* We take the radial extension of the spiral to be a large radius r_{outer} , rather than ∞ , which is an ‘infrared-type’ regularization that allows us to compute on a finite lattice, then take the thermodynamic limit. This is how the local height probabilities are evaluated, following [3].

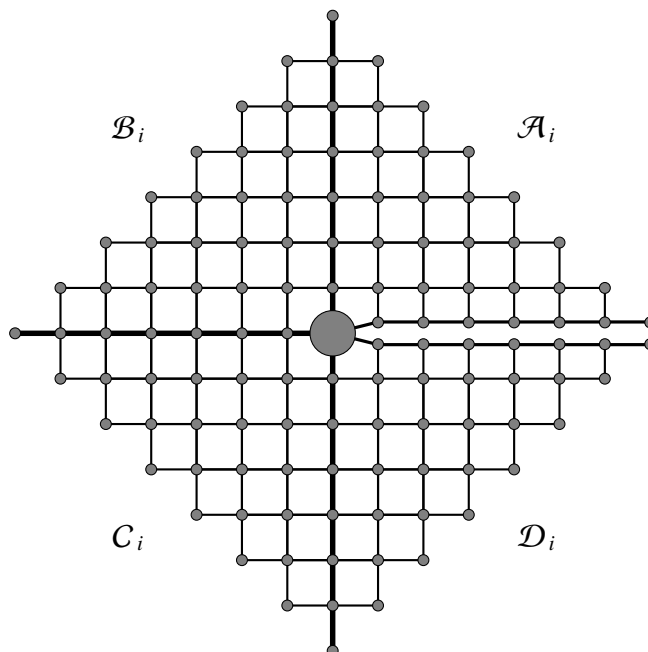


FIGURE 8.1.

8.1.2. *Regularization 2. Ultraviolet.* We remove an inner spiral of small radius r_{inner} , which is an ‘ultraviolet-type’ regularization that allows us to avoid a potential singularity near the origin in subsequent computations. One can motivate this regularization as follows. Think of the vertices on which the height variables are located as infinitesimal punctures. The height variable assigned to each vertex is distributed on the circumference. We can actually take the radii of these punctures to be finite, rather than infinitesimal. In fact, we can take the radii of different punctures to be all different, and show that the Yang-Baxter equations remain unaffected. What we wish to do here is to keep all radii infinitesimal, but take that of the vertex at the origin to be finite and small. We end up with a lattice that has ‘a hole in the middle’, as in Figure 8.1. The height variable at the center of the lattice is now distributed on the finite circumference. In a $4N$ -quadrant geometry, the circumference of the puncture at the origin becomes a finite-radius spiral, with the top and the bottom end-points identified. The small radius r_{inner} that we are interested in is the radius of this inner spiral. One can now think of taking the continuum limit as increasing the number of vertices in the lattice, while keeping r_{inner} and r_{outer} fixed.

8.2. **From a $4N$ -quadrant to an infinite spiral.** From (7.11), the one-dimensional sum in the numerator in the local height probability depends on q_N and N only through the combination $q_N^N = e^{-2\pi N \tau_N}$. We require that,

$$(8.1) \quad N \rightarrow \infty, \quad \tau_N \rightarrow 0, \quad N \tau_N = \tau_0 > 0, \quad L_N \rightarrow (NL)^N = (L')^N,$$

where τ_0 is a finite real number, and L' is a finite length in a theory with continuum degrees of freedom²¹. In this limit, the system is asymptotically close to criticality, on a spiral with $4N$ -quadrants, an inner radius r_{inner} , and an outer radius r_{outer} . In the sequel, we choose to measure distances in the theory with continuum degrees of freedom such that,

$$(8.2) \quad r_{inner} = 1, \quad r_{outer} = (L')^N$$

Choosing $\tau_N = \tau/N$, the one-dimensional configuration sum (the second factor) in the numerator of (7.11) is independent of N . In the limit (8.1), this factor remains invariant, but the first factor, as well as the denominator diverge because working in terms of the nome q_N is inadequate in the critical limit $q_N \rightarrow 1$. To deal with that, we need to perform a conjugate modulus transformation and work in terms of $p_N = e^{-2\pi/\tau_N}$. Using the identity²²,

$$(8.3) \quad \Theta_{k,l} \left(q^{\frac{1}{2}}, q \right) = q^{-l/4} \left(\frac{(m+1)}{l\tau} \right)^{\frac{1}{2}} \theta_1 \left(\pi k/l, p^{(m+1)/l} \right),$$

where the nome p , and the conjugate nome q are defined in (4.9), (7.12) can be re-written as,

$$(8.4) \quad \left(\left(\frac{3m}{2(m+1)} \right)^{1/2} \frac{\theta_1 \left(\pi j_3 / (m+1), p_N^{2/(m+1)} \right) \theta_1 \left(\pi/2, p_N \right)}{\theta_1 \left(\pi j_1 / m, p_N^{2/m} \right) \theta_1 \left(\pi j_2 / 3, p_N^{2/3} \right)} \right)^N c_{j_1 j_2 j_3} \left(q_N^N \right)$$

In the critical limit, this reduces to,

$$(8.5) \quad \left(\left(\frac{3m}{2(m+1)} \right)^{1/2} \frac{\sin \left(\pi j_3 / (m+1) \right)}{\sin \left(\pi j_1 / m \right) \sin \left(\pi j_2 / 3 \right)} \right)^N c_{j_1 j_2 j_3} \left(q_N^N \right) \sim c_{j_1 j_2 j_3} \left(q \right) = \chi_{r,s}^{Vir} \left(q \right),$$

In the first proportionality, we have dropped a constant multiplicative factor, and used $q_N = q^{1/N}$, and in the second equality, we have used (5.5–5.6).

8.3. Re-interpretation of τ . Equation (8.5) describes a partition function in a critical model in a specific geometry, with specific boundary conditions. At criticality, the effective nome $q_N^N = q$ that appears in (8.5) must be re-interpreted. Its logarithm can no longer be considered as measuring departure from criticality. From experience with calculations in finite geometries [53], we expect it to be related to ratios of the dimensions of the system. In that case, it should remain invariant under conformal transformations.

8.4. Conformal transformation 1. From an infinite spiral to an annulus. Now that we are (asymptotically) close to criticality, the system is conformally invariant, and we can use conformal transformations to bring it back to a familiar geometry. Using the conformal transformation

$$(8.6) \quad z \rightarrow z^{\frac{1}{N}} = \left(r e^{i\theta} \right)^{\frac{1}{N}},$$

²¹ We understand the limit $N \rightarrow \infty$ as $N \rightarrow N_{very\ large}$, $\tau_N \rightarrow 0$ as $\tau_N \rightarrow \tau_{very\ small}$, where $N_{very\ large}$ and $\tau_{very\ small}$ are very large and very small numbers, respectively, compute, then formally take the limits $N_{very\ large} \rightarrow \infty$, and $\tau_{very\ small} \rightarrow 0$

²² Equation (4.4 c) in [43], with appropriate changes in notation.

takes us from the spiral geometry to an annulus. The ratio $\frac{r_{outer}}{r_{inner}} = (L')^N$ which determines the radial extension of the deep spiral transforms as,

$$(8.7) \quad (L')^N \rightarrow L',$$

and we end up on an annulus that has an inner radius $r_{inner} = 1$, and an outer radius $r_{outer} = L'$.

8.5. Conformal transformation 2. From an annulus to a cylinder. We map the annulus to a cylinder of width T in the periodic direction, and height L' in the non-periodic direction, using the conformal transformation,

$$(8.8) \quad z \rightarrow w = \log z,$$

which puts us on a strip with,

$$(8.9) \quad 2\pi H = \log L', \quad T = 2\pi,$$

where the factor 2π in $2\pi H$ is chosen to simplify the notation in the sequel. Since we have maintained periodic boundary conditions in the angular direction, this strip is equivalent to a cylinder of aspect ratio H . The finite size that appears in the computations of the characters, as given in [53] is parameterized by the nome $q_N^N = q = e^{-4\pi\tau/(m+1)}$, where $\tau = T/(2\pi H)$. In our case,

$$(8.10) \quad \tau = \frac{2\pi}{2\pi H} = \frac{1}{H},$$

in complete agreement with the result of Saleur and Bauer [53]. The factor raised to a power N in (7.1) is such that, under the first conformal transformation, this power is canceled, and we end up with a finite numerical factor that, for the purposes of this work, can be ignored.

9. POSTSCRIPT

9.1. Surface critical exponents in cyclic solid-on-solid models. In [56], Seaton and Nienhuis used the spiral geometry that interpolates off-critical models on a plane and critical models on a cylinder, as proposed in [57] and reproduced in the present work, to compute surface critical exponents in cyclic solid-on-solid models.

9.2. q -Virasoro algebra. In [58], Shiraishi, Kubo, Awata and Odaka obtained a q -deformed version of the Virasoro algebra that extends the known Virasoro algebra off-criticality. The identification in [37] of Virasoro characters as the essential factors in Regime-III local height probabilities was surprising when first discussed in the 1980's because, at the time, such a deformation was not known. Now that we know that this deformation exists, the appearance of Virasoro characters off-criticality, should be less of a surprise. The interpolation obtained in this paper is a concrete way to see how the same object, $X(a|b, b \pm 1|q)$ appears at criticality as a partition function on a cylinder, and also off-criticality as the essential factor in a local height probability.

9.3. Two ways to introduce a scale lead to identical results. A critical system is characterized by the absence of a characteristic mass or length scale. A characteristic scale can be introduced either **1.** By varying a physical parameter such as the temperature away from its critical value, or **2.** By introducing finite size effects. The effects of **1** and **2** on the same initial critical system are physically distinct. However, we know from [37, 40, 53] that the off-critical one-point functions in regime-III restricted solid-on-solid models [3], and the partitions functions of the corresponding minimal conformal field theories on a cylinder, can be expressed (up to an overall normalization) in terms of the same characters of Virasoro degenerate irreducible highest-weight modules, which are q -series in an indeterminate $q = e^{-4\pi\tau/(m+1)}$. Off criticality, on a plane, τ is a parameter that measures departure from criticality. At criticality, on a cylinder, τ is the aspect-ratio (circumference to width) of the cylinder²³.

9.4. Interpretation. An interplay of geometry and physics. One way to understand the above result is to say that, if we ignore normalization factors that do not carry information about the statistical mechanics, the essential part of the the local height probability $P(a|b, b \pm 1|q)$, namely the one-dimensional sum $X(a|b, b \pm 1|q)$ is a mathematical object that can be interpreted in two different ways, **1.** as an off-critical one-point function on a plane, τ -away from criticality, and **2.** as a critical partition function on a cylinder of aspect-ratio τ . The fact that the same q -series appears in these two physically-distinct settings points to an interplay between the geometry of the surface that a model lives on, and the physics of the model, in the sense of how far it is from criticality. To understand this interplay better, we extend the definition of the off-critical local height probabilities from the 4-quadrant plane geometry to a $4N$ -quadrant spiral geometry, then formally take $N \in \mathbb{R}$, to obtain an object that interpolates the off-critical local height probabilities on a plane and the partition functions on a finite cylinder which are Virasoro characters.

9.4.1. Constant- $(N\tau)$ curves. Consider the parameter space with coordinates (N, τ) , where $1 \leq N < \infty$ parameterizes the geometry of the configuration that the model lives on, and $0 < \tau < \infty$ parameterizes its departure from criticality. Our result is that this parameter spaces is foliated by constant- $(N\tau)$ curves, $N\tau = \tau_0 \in \mathbb{R}$, that we call τ_0 -curves, where $0 < \tau_0 < \infty$ is constant, and the local height probability is invariant, as a q -series, on a τ_0 -curve. At the $(1, \tau)$ -end of a τ_0 -curve, the q -series has the interpretation of a local height probability. At the $(N \rightarrow \infty, \tau \rightarrow 0)$ -end, it has the interpretation of critical partition function on a cylinder, which following Saleur and Bauer is a Virasoro character [53]. As q -series, for $\tau = -\log q = \tau_0$, these two limits are equal.

9.5. Epilogue. The starting point of this work is an observation by Date, Jimbo, Miwa and Okada [37], followed by another observation by Saleur and Bauer [53]. In [40], Date *et al.* conclude a review of their work on the subject with ‘*Modular invariance plays two different roles in the 2D lattice systems. Are they totally unrelated to each other? It is unbelievable. Then what is the structure governing both? We stop the lecture with this question.*’ In this work, we have argued that local height probabilities on a spiral geometry are interpolating objects, with well-defined modular properties, that reduce to each of the objects referred to by Date *et*

²³ As in [37, 40, 53], we restrict our attention in the present work to regime-III restricted solid-on-solid models and the corresponding minimal conformal field theories. Our result is expected to extend to models other solid-on-solid models. Following the appearance of the first version of this work [57], it was extended in [56] to cyclic solid-on-solid models.

al. in appropriate limits. We wish to argue that the existence of these interpolating objects, and their functional dependence on the winding number N and departure from criticality τ , realizes the relation forecast by Date *et al.*

ACKNOWLEDGEMENTS

I would like to thank H Saleur for a discussion on [53] in 1988, and J B Zuber for a discussion on [51] in 2017. This work was supported by the Australian Research Council.

REFERENCES

- [1] R J Baxter, *Hard hexagons: exact solution*, Journal of Physics A: Mathematical and General **13.3** (1980) L61–L70
- [2] R J Baxter, *Roger-Ramanujan Identities in the hard Hexagon Model*, Journal of Statistical Physics **26.3** (1981) 427–452
- [3] G E Andrews, R J Baxter, and P J Forrester, *Eight-vertex SOS model and generalized Rogers-Ramanujan-type identities*, Journal of Statistical Physics **35.3** (1984) 193–266
- [4] I S Gradshteyn and I M Ryzhik, *Table of integrals, series, and products*, Academic Press (1994), ISBN-10: 012294755X, ISBN-13: 978-0122947551
- [5] D Friedan, Z Qiu, and S Shenker, *Conformal invariance, unitarity, and critical exponents in two dimensions*, Physical Review Letters **52.18** (1984) 1575–1578
- [6] D Friedan, Z Qiu, and S Shenker, *Conformal invariance, unitarity and two dimensional critical exponents*, 419–449, in *Vertex operators in mathematics and physics*, Mathematical Sciences Research Institute Publications (Book 3), J Lepowsky (Editor), S Mandelstam (Editor), and I Singer (Editor), Springer, New York, NY (1985) ISBN 0387961216
- [7] A A Belavin, A M Polyakov, and A B Zamolodchikov, *Infinite conformal symmetry of critical fluctuations in two dimensions*, Journal of Statistical Physics **34.5** (1984) 763–774
- [8] A A Belavin, A M Polyakov, and A B Zamolodchikov, *Infinite conformal symmetry in two-dimensional quantum field theory*, Nuclear Physics **B 241** (1984) 333–380
- [9] P J Forrester and R J Baxter, *Further exact solutions of the eight-vertex SOS model and generalizations of the Rogers-Ramanujan identities*, Journal of Statistical Physics **38.3** (1985) 435–472
- [10] V Pasquier, *Two-dimensional critical systems labelled by Dynkin diagrams*, Nuclear Physics **B 285** (1987) 162–172
- [11] V Pasquier, *Exact solubility of the D_n series*, Journal of Physics A: Mathematical and General **20.4** (1987) L217–L220
- [12] V Pasquier, *D_n models: local densities*, Journal of Physics A: Mathematical and General **20.4** (1987) L221–L226
- [13] C Itzykson, H Saleur, and J- Zuber, Editors, *Conformal invariance and applications to statistical mechanics*, World Scientific Publishing Company (1998) Singapore, ISBN-10: 9971506068, ISBN-13: 978-9971506063
- [14] V Pasquier, *Lattice derivation of modular invariant partition functions on the torus*, Journal of Physics A: Mathematical and General **20.18** (1987) L1229–L1237
- [15] B Nienhuis, *Critical behavior of two-dimensional spin models and charge asymmetry in the Coulomb gas*, Journal of Statistical Physics **34.5-6** (1984) 731–761

- [16] B Nienhuis, *Two-dimensional critical phenomena and the Coulomb Gas*, in *Phase Transitions and Critical Phenomena*, C Domb, M Green, and J L Lebowitz, Editors, volume **11** (1987) Academic Press, ISBN-13: 978-0122203114, ISBN-10: 0122203119
- [17] A Kuniba and T Yajima, *Local state probabilities for an infinite sequence of solvable lattice models*, *Journal of Physics A: Mathematical and General* **21.2** (1988) 519–527
- [18] A Kuniba and T Yajima, *Local state probabilities for solvable restricted solid-on-solid models: A_n , D_n , $D_n^{(1)}$, and $A_n^{(1)}$* , *Journal of statistical physics* **52.3–4** (1988) 829–883
- [19] P A Pearce and K A Seaton, *Solvable hierarchy of cyclic solid-on-solid lattice models*, *Physical Review Letters* **60.14** (1988) 1347–1350
- [20] P A Pearce K A Seaton, *Exact solution of cyclic solid-on-solid lattice models*, *Annals of Physics* **193.2** (1989) 326–366
- [21] R J Baxter, *Dimers on a rectangular lattice*, *Journal of Mathematical Physics* **9.4** (1968) 650–654
- [22] R J Baxter, *Variational approximations for square lattice models in statistical mechanics*, *Journal of Statistical Physics* **19.5** (1978) 461–478
- [23] R J Baxter, *Corner transfer matrices*, *Physica* **106A** (1981) 18–27
- [24] R J Baxter, *Exactly Solved Models in Statistical Mechanics*, Academic Press, 1982, ISBN 0120831805
- [25] G E Andrews, *The hard-hexagon model and Rogers-Ramanujan type identities*, *Proceedings of the National Academy of Sciences USA* **78.9** (1981) 5290–5292
- [26] A Rocha-Caridi, *Vacuum vector representations of the Virasoro algebra*, *Vertex operators in mathematics and physics* **3**, Springer, (1985) 451–473
- [27] R Kedem, T R Klassen, B M McCoy, and E Melzer, *Fermionic quasi-particle representations for characters of $G_1^{(1)} \times G_1^{(1)}/G_2^{(1)}$* , *Physics Letters B* **304.3–4** (1993) 263–270, hep-th/9211102
- [28] R Kedem, T R Klassen, B M McCoy, and E Melzer, *Fermionic sum representations for conformal field theory characters*, *Physics Letters B* **307.1–2** (1993) 68–76, hep-th/9301046
- [29] A Berkovich, *Fermionic counting of RSOS states and Virasoro character formulas for the unitary minimal series $M(v, v+1)$: Exact results*, *Nuclear Physics B* **431.1–2** (1994) 315–348, hep-th/9403073
- [30] A Berkovich and B M McCoy, *Continued Fractions and Fermionic Representations for Characters of $M(p, p')$ minimal models*, *Letters in Mathematical Physics* **37** (1996) 49–66, arXiv:hep-th/9412030
- [31] S O Warnaar, *Fermionic solution of the Andrews-Baxter-Forrester model. I. Unification of TBA and CTM methods*, *Journal of statistical physics* **82.3-4** (1996) 657–685, hep-th/9501134
- [32] S O Warnaar, *Fermionic solution of the Andrews-Baxter-Forrester model. II. Proof of Melzer’s polynomial identities*, *Journal of statistical physics* **84.1** (1996) 49–83, hep-th/9508079
- [33] O Foda, K S M Lee, and T A Welsh, *A Burge tree of Virasoro-type polynomial identities*, *International Journal of Modern Physics A* **13** (1998) 4967–5012, arXiv:q-alg/9710025
- [34] O Foda, K S M Lee, Y Pugai, and T A Welsh, *Path generating transforms*, in *q-Series from a contemporary perspective*, (South Hadley, MA, 1998), 157–186, *Contemporary Mathematics* **254**, American Mathematical Society, Providence, RI, 2000, arXiv:math/9810043

- [35] O Foda and T A Welsh *On the combinatorics of Forrester-Baxter models*, in *Physical combinatorics* (Kyoto, 1999), 49–103, Progress in Mathematics **191**, Birkhauser, Boston, MA, 2000, arXiv:math/0002100
- [36] T A Welsh, *Fermionic expressions for minimal model Virasoro characters*, Memoirs of the American Mathematical Society (2005) **175 N 827** 1–160, arXiv:math/0212154
- [37] A Date, M Jimbo, T Miwa, and M Okado, *Automorphic properties for local height probabilities for integrable solid-on-solid models*, Physical Review **B 35** (1987) 2105–2107
- [38] D Mumford, *Tata Lectures on Theta I*, Progress in Mathematics **28** (1983) Birkhauser ISBN-10: 3764331097, ISBN-13: 978-3764331092
- [39] V G Kac and D H Peterson, *Infinite-dimensional Lie algebras, theta functions and modular forms*, Advances in Mathematics **53.2** (1984) 125–264
- [40] A Date, M Jimbo, T Miwa, and M Okado, *Solvable lattice models*, in *Proceedings in Symposia in Pure Mathematics* **49**, Part I (1989) 295–332
- [41] P Goddard, A Kent, and D Olive, *Virasoro algebras and coset space models*, Physics Letters **152.1–2 B** (1985) 88–92
- [42] P Goddard, A Kent, and D Olive, *Unitary representations of the Virasoro and super-Virasoro algebras*, Communications in Mathematical Physics **103.1** (1986) 105–119
- [43] A Date, M Jimbo, A Kuniba, T Miwa, and M Okado, *Exactly solvable SOS models: Local height probabilities and theta function identities*, Nuclear Physics **B 290** [FS20] (1987) 231–273
- [44] A Date, M Jimbo, A Kuniba, T Miwa, and M Okado, *Exactly solvable SOS models II: Proof of the star triangle relations and combinatorial identities*, in *Advanced Studies in Pure Mathematics* **16** (1988) *Conformal field theory and solvable lattice models*, 17–122
- [45] D A Huse, *Exact exponents for infinitely many new multicritical points*, Physical Review **B 30** (1984) 3908–3915
- [46] G von Gehlen and V Rittenberg, *The spectra of quantum chains with free boundary conditions and Virasoro algebras*, Journal of Physics **A: Mathematical and General** **19.10** (1986) L631–L635
- [47] N Boccarda and G Sarma, *Does magnetic surface order exist?*, Journal de Physique Lettres **35.7-8** (1974) 95–97
- [48] T Burkhardt and I Guim, *Finite-size scaling of the quantum Ising chain with periodic, free, and antiperiodic boundary conditions*, Journal of Physics **A: Mathematical and General** **18.1** (1985) L33–L37
- [49] J L Cardy, *Operator content of two-dimensional conformally invariant theories*, Nuclear Physics **B 270** [FS10] (1986) 186–204
- [50] ‘*Superstrings. The first 15 years of superstring theory*’, Volumes 1 and 2, J H Schwarz (Editor) World Scientific, Singapore, 1985, ISBN-10: 9971978679
- [51] J L Cardy, *Effect of boundary conditions on the operator content of two-dimensional conformally invariant theories*, Nuclear Physics **B 275** [FS17] (1986) 200–218
- [52] H Saleur, *Conformal invariance for polymers and percolation*, Journal of Physics **A: Mathematical and General** **20.2** (1987) 455–470
- [53] H Saleur and M Bauer, *On some relations between local height probabilities and conformal invariance*, Nuclear Physics **B 320** (1989) 591–624
- [54] C J Hamer, G R W Quispel, and M T Batchelor, *Conformal anomaly and surface energy for Potts and Ashkin-Teller quantum chains*, Journal of Physics **A: Mathematical and General** **20.16** (1987) 5677–5693

- [55] F C Alcaraz, M N Barber, and M T Batchelor, *Conformal invariance and the spectrum of the XXZ chain*, Physical Review Letters **58.8** (1987) 771–774
- [56] K A Seaton and B Nienhuis, *Surface critical phenomena and cylindrical partition functions for the CSOS model*, Nuclear Physics **B 384** (1992) 507–522
- [57] O Foda, *Off-critical local height probabilities and critical partition functions on a cylinder*, University of Nijmegen preprint (1991)
- [58] J Shiraishi, H Kubo, H Awata, and S Odake, *A Quantum Deformation of the Virasoro Algebra and the Macdonald Symmetric Functions*, Letters in Mathematical Physics **38** (1996) 33–51, [arXiv:q-alg/9507034](https://arxiv.org/abs/q-alg/9507034)

SCHOOL OF MATHEMATICS AND STATISTICS, UNIVERSITY OF MELBOURNE, PARKVILLE, VICTORIA 3010, AUSTRALIA.
E-mail address: omar.foda@unimelb.edu.au